2nd URSI AT-RASC, Gran Canaria, 28 May – 1 June 2018

1D Localization of Mobile Stochastic EM Sources with Variable Radiated Power using Two-Stage Neural Model

Zoran Stanković[(1)], Nebojša Dončov[(1)], Ivan Milovanović[(2)], Biljana Stošić[(1)], Bratislav Milovanović[(2)] and Johannes Russer[(2)]
(1) University of Niš, Faculty of Electronic Engineering, Aleksandra Medvedeva 14
(2) Singidunum University, Danijelova 32, 11000 Beograd, Serbia
(3) Technical University of Munich, Arcisstr. 21(0509)/III, 80333 München

Abstract

In this paper, a cascade two-stage neural model is proposed for 1D DoA estimation of mobile stochastic EM sources with variable radiated power. Architecture of the neural model is based on MLP neural networks whose number is determined by the dimension of the linear antenna array at the receiver. Model accuracy is illustrated on the example of two uncorrelated EM sources whose radiated powers are fluctuated during their movement.

1. Introduction

The presence of sources of electromagnetic interference (EMI) of either deterministic or stochastic radiation, can severely degrade the performances of today wireless communication systems [1-3]. Their negative impact can be suppressed by a spatial signal filtering using adaptive antenna arrays [1]. Adaptive beamforming of such antenna arrays is usually based on the Direction of Arrival (DoA) estimation techniques commonly based on the super-resolution algorithms such as MUSIC and its modifications [1,4]. However, the implementation of these algorithms may be confronted with hardware constraints of different types so they may not be suited for real-time applications. Therefore, the usage of artificial neural networks (ANNs) in the DoA estimation process was proposed in [5-7] as a good real-time alternative.

Multilayer perceptron (MLP) neural networks were used by the authors of this paper for the realization of a neural model for 2D DoA estimation of deterministic [8] and 1D DoA estimation of stochastic sources of electromagnetic (EM) radiation [9,10]. For the stochastic EMI, either uncorrelated [9] or partially correlated sources [10] were considered. It was shown that in both stochastic cases, it is sufficient to take only values of the first row of spatial correlation matrix obtained by an antenna array sampling, for the training of a neural model that provides 1D DoA estimation with an accuracy close to super-resolution algorithms but with much faster run-time.

In all previous cases [9-10], it was assumed the stochastic EM sources are with constant radiation power during their movement. Here, we consider the more general scenario in which movable stochastic EM sources are with fluctuated radiation power. Cascade two-stage neural MLP model is proposed to efficiently perform 1D localization of such mobile stochastic EM sources. Model accuracy is illustrated on the example of two uncorrelated EM sources with variable radiated power.

2. Stochastic Source Radiation Model

Initial assumption in our research presented here, as in previous papers [9-10], is that a stochastic EM source in the far-field can be represented by a short dipole, fed by stochastic current. Sources are moving in the azimuth plane along the straight 1D path and an orientation of each dipole representing one source can change during the movement allowing to simulate the fluctuation of stochastic source radiation power in time. Mutual level of correlation between the stochastic EM sources is expressed through the correlation between fed currents of dipoles as [2,3]:

$$\mathbf{c}^{I}(\omega) = \lim_{T\to\infty} \frac{1}{2T}\left[\mathbf{I}(\omega)\mathbf{I}(\omega)^{H}\right] \tag{1.}$$

where $\mathbf{I} = [I_1, I_2, \ldots, I_S]^{\mathrm{T}}$ is a vector of fed current of dipoles and S is the number of stochastic EM sources. By using the Green function in free space:

$$\mathbf{M}^{(\mathrm{Y})} = \mathbf{M}^{(\mathrm{Y})}(\theta_1,\ldots,\theta_s,\ldots,\theta_S,\varphi_1,\ldots,\varphi_s,\ldots,\varphi_S,r_1,\ldots,r_s,\ldots,r_S) = \frac{jz_0}{2\pi}\left[\frac{F_1(\theta_1,\varphi_1)e^{jkr_1}}{r_1}\cdots\frac{F_s(\theta_s,\varphi_s)e^{jkr_s}}{r_s}\cdots\frac{F_S(\theta_S,\varphi_S)e^{jkr_S}}{r_S}\right] \tag{2.}$$

the electric field in a particular sampling point Y in the far-field, can be calculated as:

$$E^{(\mathrm{Y})}(\theta_1,\ldots,\theta_s,\ldots\theta_S,\varphi_1,\ldots,\varphi_s,\ldots\varphi_S,r_1,\ldots,r_s,\ldots r_S) = \mathbf{M}^{(\mathrm{Y})}\mathbf{I} \tag{3.}$$

In Eq. (2), $F_s(\theta,\varphi)$ is the radiation pattern of the s-th stochastic EM source, r_s is the distance between s-th stochastic EM source and the sampling point, z_0 is the impedance of free space, k is the phase constant ($k=2\pi/\lambda$) and θ and φ are angles used to describe the angular position of stochastic EM source relative to the particular sampling point in the far-field.

Spatial correlation matrix in the far field is obtained by sampling the signals using a uniform linear antenna array with M sensors (Fig. 1, the scenario of movement and DoA estimation of two stochastic sources). Axis of antenna array is parallel to the direction of movement of stochastic EM sources, while the positions of sensors are described by points Y_1, Y_2, ..., Y_M. Sensors are at equal mutual distance y_d.

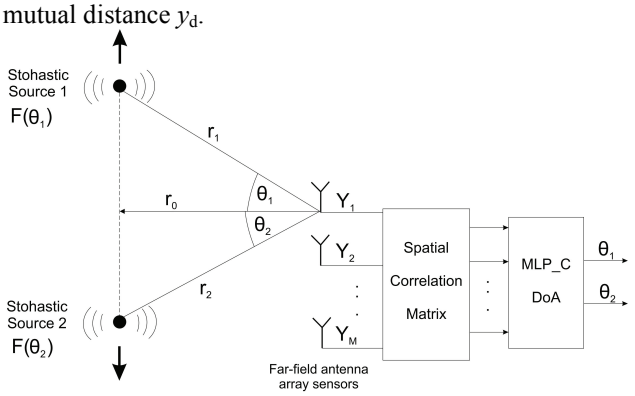

Figure 1. Angular position of mobile stochastic EM sources with different signal levels with respect to the sensors of antenna array performing the sampling of the received signals

Combining Eqs. (1), (2) and (3), the correlation matrix in the far field can be expressed as:

$$\tilde{\mathbf{C}}_E[i,j] = \mathbf{M}^{(Y_i)}\mathbf{c}^I(\mathbf{M}^{(Y_j)})^H \quad i=1,...,M \;\; j=1,...,M \quad (4.)$$

As we initially assumed that EM sources are moving only in azimuth plane, angle φ is equal to zero for any position of the stochastic EM source and the matrix $\mathbf{c}^I$. is a unit matrix due to uncorrelated sources. Therefore, the azimuth angular position and distance of s-th stochastic EM source relative to m-th antenna array sensor is:

$$\theta_s^{(m)} = \arctan\left[\tan\theta_s^{(1)} - \frac{(m-1)\cdot y_d}{r_0}\right] \quad r_s^{(m)} = \frac{r_0}{\cos\theta_s^{(m)}} \quad (5.)$$

Angle θ_s represents the azimuth angular position of s-th source relative to the antenna array and it can be determined as angle position in relation to the first sensor of the antenna array when $\theta_s = \theta_s^{(1)}$. Using Eqs. (2), (4) and (5) for given angular position of radiation source we may determine the mapping function **M**, and afterwards also the elements of the correlation matrix using Eq. (4). Fig.1 illustrates the movement of two stochastic EM sources (S = 2) with variable radiated power. For the development of neural model the correlation matrix normalized with the first matrix element is used:

$$\mathbf{C}_E = \frac{1}{\tilde{C}_{E11}}\cdot\tilde{\mathbf{C}}_E \quad (6.)$$

In this case, the changes in radiation power of s-th stochastic source are modeled through a variable relative ratio of radiation pattern functions:

$$p_s(\theta_s,\varphi_s) = 10\log\left[\frac{F_s(\theta_s,\varphi_s)}{F_1(\theta_1,\varphi_1)}\right] \quad (7.)$$

3. Neural Network Model

Cascade neural model, proposed here, has two stages (see Fig. 2). As shown in [9], it is sufficient to consider only elements from the first row of correlation matrix $\mathbf{C}_E$ for the training of MLP model performing 1D DoA estimation of uncorrelated radiation sources whose radiation powers are constant during the movement. Accordingly, the fundamental task of the first stage model is to do the mapping of the first row of the correlation matrix $\mathbf{x}(\mathbf{C}_E) = [C_{ij}]_{1\times M}, i=1, j\in\{1,\ldots,M\}$, sampled under condition of variable radiation power of stochastic sources during their movement, to the elements of the first row of the correlation matrix $\mathbf{x}(\overline{\mathbf{C}}_E) = [\overline{C}_{ij}]_{1\times M}, i=1, j\in\{1,\ldots,M\}$ that would be obtained by sampling under condition that radiation powers are constant while sources are moving. The first stage model contains M-1 MLP networks (Fig.3.a) where m-th network marked as MLP_C$_{1m}$ performs mapping:

$$\overline{C}_{1m} = f_{MLP\_C1m}(\mathbf{x}(\mathbf{C}_E)) \quad m\in\{2,\ldots,M\} \quad (8.)$$

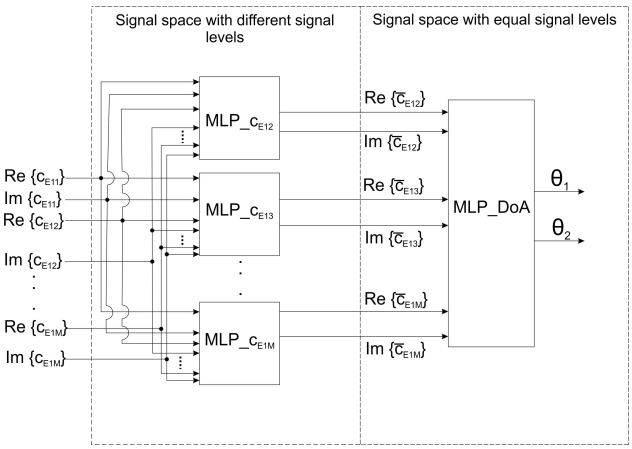

Figure 2. Architecture of the two-stage cascade neural model (MLP_C)

As matrix $\mathbf{C}_E$ is normalized relative to (1,1) element mapping to $\overline{C}_{E11}$ element is not considered as this element has unit value and therefore it is not used in the second stage model for DoA estimation.

The second stage realized through MLP_DoA network (Fig.3.b) has a task to, based on elements of the first row of the correlation matrix $\overline{\mathbf{C}}_E$ determine the azimuth positions of stochastic sources:

$$[\theta_1\;\theta_2]^T = f_{MLP\_DoA}(f_{MLP\_C12}(\mathbf{x}(\mathbf{C}_E)),\ldots,f_{MLP\_C1M}(\mathbf{x}(\mathbf{C}_E))) \quad (9.)$$

MLP networks used in cascade neural model can be described by the following function:

$$\mathbf{y}_l = F(\mathbf{w}_l\mathbf{y}_{l-1} + \mathbf{b}_l) \quad l=1,2,\ldots,H \quad (10.)$$

where $\mathbf{y}_{l-1}$ vector represents the output of (l-1)-th hidden layer, $\mathbf{w}_l$ is a connection weight matrix among (l-1)-th and

l-th hidden layer neurons, $\mathbf{b}_l$ is a vector containing biases of l-th hidden layer neurons and H is number of hidden layers. F is the activation function of neurons in hidden layers and in this case it is a hyperbolic tangent sigmoid transfer function $F(u) = (e^u - e^{-u})/(e^u + e^{-u})$. Real and imaginary parts of correlation matrix elements are separately brought at the input of the network. Therefore, the input layer of each MLP_C$_{1m}$ network has the form $\mathbf{y}_0 = [\mathrm{Re}\{\mathbf{x}(\mathbf{C}_E)\}\ \mathrm{Im}\{\mathbf{x}(\mathbf{C}_E)\}]_{1\times 2M}$, while the input layer of the MLP_DoA network has the form $\mathbf{y}_0 = [\mathrm{Re}\{\mathbf{x}(\overline{\mathbf{C}}_E)\}\ \mathrm{Im}\{\mathbf{x}(\overline{\mathbf{C}}_E)\}]_{1\times 2(M-1)}$. The output of the MLP_C$_{1m}$ neural network model is given as $[\mathrm{Re}\{C_{1m}\}\ \mathrm{Im}\{C_{1m}\}]^T = \mathbf{y}_{H+1} = \mathbf{w}_{H+1}\mathbf{y}_H$, while output of the MLP_DoA network model is given as $[\theta_1\ \theta_2]^T = \mathbf{w}_{H+1}\mathbf{y}_H$. In these notations $\mathbf{w}_{H+1}$ is a connection weight matrix between neurons of the last hidden layer and neurons in the output layer. During the neural network training, weight matrices $\mathbf{w}_1$, $\mathbf{w}_2$,…, $\mathbf{w}_H$, $\mathbf{w}_{H+1}$ and biases values are optimized to achieve the desired mapping accuracy. The general notation used to describe MLP neural model used in first or second model stage is MLPH-N_1-…-N_i-…-N_H where H is the total number of hidden MLP network layers and N_i is the total number of neurons in the i-th hidden layer.

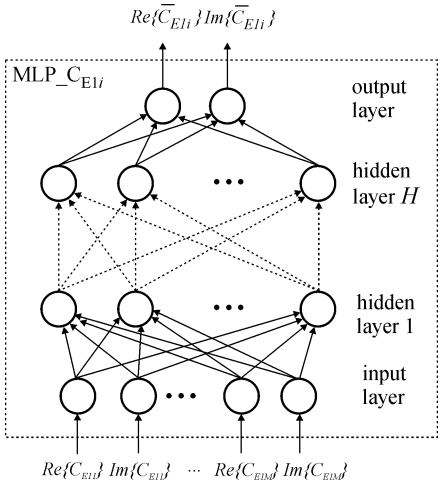

Figure 3. MLP architecture used in MLP_C$_{1m}$ and MLP_DoA networks

4. Modeling Results

A MLP_C neural model, whose architecture is shown in the section 3, is used to determine the angular position in the azimuth plane of two uncorrelated stochastic EM sources with variable radiated power. Sources are moving along a straight line trajectory that is distant from the sampling place at r_0 = 1000 m. Parameter p, that gives information about the change of difference between signal level of two sources due to variation of their radiation powers, varies in the range 0 dB ≤ p ≤ 10 dB. Signal is sampled by the antenna array consisting of M=4 sensor elements at the frequency f = 28 GHz. The mutual distance between the neighboring antenna sensors is y_d =0.5λ. Implementation, training and testing of neural models were conducted in MATLAB software environment. Quasi-Newton training method with the prescribed accuracy 10^{-4} was used.

Training and testing of MLP_C models are carried out in two steps. In the first step, the training and testing of MLP networks of the first stage, MLP_C$_{12}$, MLP_C$_{13}$ and MLP_C$_{14}$, are conducted for the different number of neurons in hidden layers. Based on relations in Eqs (2), (4) and (7), an inverse mapping is established in relation to the mapping given in Eq. (9)

$$\mathbf{C}_E^t = f_{DoA}^{-1}\left(\theta_1^t, \theta_1^t, p\right) \qquad (10.)$$

Table 1. Testing results for four MLP_C$_{E12}$ neural networks with the best test statistics

MLP network	WCE [%]	ATE [%]	r^{PPM}
MLP2-23-23	11.67	1.26	0.9972
MLP2-22-20	13.63	1.33	0.9969
MLP2-22-22	12.24	1.34	0.9968
MLP2-18-18	13.00	1.34	0.9966

Table 2. Testing results for four MLP_C$_{E13}$ neural networks with the best test statistics

MLP network	WCE [%]	ATE [%]	r^{PPM}
MLP2-23-23	11.57	1.68	0.9961
MLP2-18-18	12.84	2.08	0.9941
MLP2-22-20	13.12	1.97	0.9947
MLP2-22-22	13.03	1.71	0.9959

Table 3. Testing results for four MLP_C$_{E14}$ neural networks with the best test statistics

MLP network	WCE [%]	ATE [%]	r^{PPM}
MLP4-23-23	26.62	2.72	0.9893
MLP4-22-20	20.76	3.10	0.9863
MLP4-18-14	20.98	3.44	0.9831
MLP4-18-14	19.40	3.38	0.9842

Table 4. Testing results for six MLP_DoA neural networks with the best test statistics

MLP network	WCE [%]	ATE [%]	r^{PPM}
MLP2-23-23	7.76	0.79	0.9990
MLP2-16-16	7.98	0.81	0.9990
MLP2-18-18	8.60	0.80	0.9990
MLP2-18-16	8.19	0.80	0.9990
MLP2-22-20	8.16	0.81	0.9990
MLP2-22-22	8.08	0.77	0.9990

By using this mapping, the training and testing sets for MLP_C$_{1m}$ networks are generated and they are in the form $\{\mathbf{x}^t(\mathbf{C}^t_E(\theta^t_1, \theta^t_2, p^t)), \mathrm{Re}\{\overline{C}_{E1m}\}, \mathrm{Im}\{\overline{C}_{E1m}\})\}$. Thereby the following distribution of samples is used

$$\left\{\begin{array}{l}(\mathbf{x}^t(\mathbf{C}^t_E(\theta^t_1,\theta^t_2,p^t)),\theta^t_1,\theta^t_2)\,| \\ \theta^t_1 \in [-30:\theta^t_{step}:30],\ \theta^t_2 \in [-30:\theta^t_{step}:30],\ \theta^t_1 > \theta^t_2, \\ c^t \in [0:p^t_{step}:10]\end{array}\right\} \qquad (11.)$$

where values used to generate training and testing sets are θ^t_{step} = 1, p^t_{step} = 1 and θ^t_{step} = 1.3, p^t_{step} = 1.3 respectively. 20130 training samples and 8648 testing samples were

generated by using Eqs. (10) and (11). For all three networks used in MLP_C models we chose MLP2-23-23 arhitecture as it provides the best testing results (Table 1. - 3.). Testing metrics is WCE - worst case error, ACE - average test error and correlation coeficient r^{PPM}.

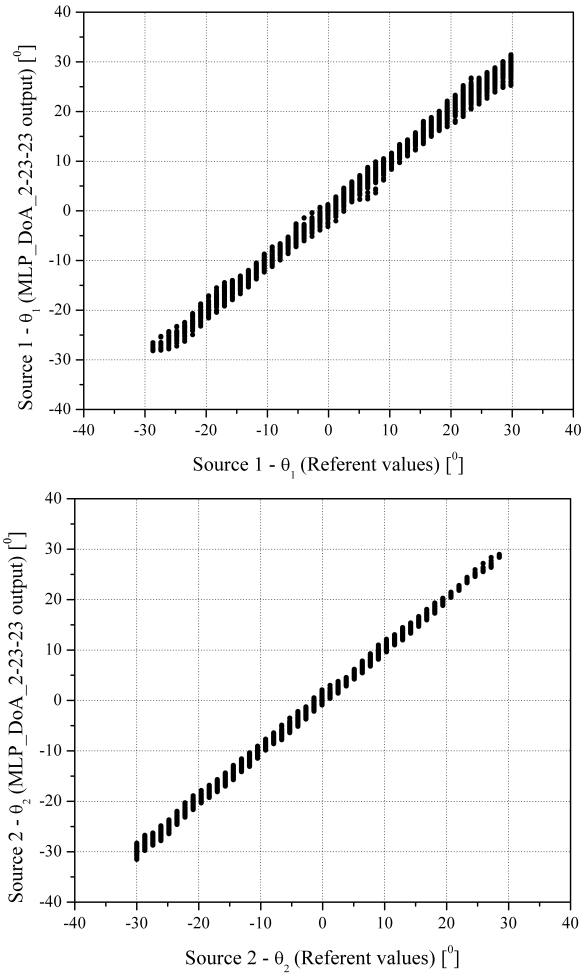

Figure 4. Scattering diagram of MLP_DoA_2-23-23 model on test set: θ_1 output and θ_2 output

In the second step, training and testing of MLP_DoA network in the second stage are conducted. By using mapping and distribution given by Eqs. (10) and (11), respectively, as well as values of outputs of MLP_C$_{1m}$ networks that they give on combination of input values obtained by using the distribution from Eq. (11), the training and testing sets of the form $\left\{\left(\mathbf{x}^t(\overline{\mathbf{C}}_E^t(\theta_1^t,\theta_2^t)),\theta_1^t,\theta_2^t\right)\right\}$ are obtained with the same number of samples as for the first stage model. Similarly as in the first step, here we also chose MLP2-23-23 network for MLP_DoA network, as it provides the best testing results (Table 4.) Scattering diagran of the MLP_C model realized by using MLP2-23-23 networks (MLP_DoA_2-23-23) is shown in Fig. 4.

5. Conclusion

MLP neural network architecture, already proven for 1D localization of mobile stochastic EM sources with constant radiation powers, is used here for a realization of cascade two-stage neural model, capable to perform 1D DoA estimation of uncorrelated EM sources with fluctuated radiated powers. Proposed model gives results of acceptable accuracy.

6. Acknowledgements

This work has been supported by the Ministry for Education, Science and Technological Development of Serbia, projects number TR32052 and TR32054.

7. References

1. B. Allen, M. Ghavami, *Adaptive Array Systems: fundamentals and applications*, Wiley, 2005

2. J.A. Russer, T. Asenov and P. Russer, "Sampling of stochastic electromagnetic fields", *IEEE MTT-S International Microwave Symposium Digest*, Montreal, Canada, pp. 1-3, 2012.

3. J.A. Russer, P. Russer, "Modeling of Noisy EM Field Propagation Using Correlation Information", *IEEE Transactions on Microwave Theory and Techniques*, Volume 63, Issue 1, pp.76-89, 2015

4. R. Schmidt, "Multiple emitter location and signal parameter estimation", *IEEE Transactions on Antennas and Propagation*, vol. 34, no. 3, pp. 276-28, 1986.

5. S. Haykin, *Neural Networks*, New York, IEEE, 1994.

6. Q. J. Zhang, K. C. Gupta, *Neural networks for RF and microwave design,* Artech House*,* Boston, MA, 2000.

7. A. H. El Zooghby, C. G. Christodoulou, M. Georgiopoulos, "A neural network based smart antenna for multiple source tracking", *IEEE Trans. on Antennas and Propagation*, Vol. 48, no. 5, pp. 768 – 776, 2000.

8. M. Agatonović, Z. Stanković, N. Dončov, L. Sit, B. Milovanović, T. Zwick, "Application of artificial neural networks for efficient high-resolution 2D DOA estimation", *Radioengineering*, Vol. 21, No. 4, pp. 1178-1186, 2012.

9. Z. Stankovic, N. Doncov, I. Milovanović, B. Milovanović, "Neural network model for efficient localization of a number of mutually arbitrary positioned stochastic EM sources in far-field", *Proc. of the 12th Symposium on Neural Network Applications in Electrical Eng. – NEUREL 2014*, Beograd, Serbia, pp. 41-44, 2014.

10. Z. Stanković, N. Doncov, I. Milovanović, M. Sarevska, B. Milovanović, "Neural Model for Far-Field 1D Localization of Mobile Stochastic EM Sources with Partially Correlated Radiation", *Proceedings of the International Scientific Conference on Information Technology and Data Related Research - SINTEZA 2017*, Belgrade, Serbia, pp. 169-175, 2017.